



ELSEVIER

Structural properties of GaAs/Ge heterostructures as a function of growth conditions

L. Lazzarini^a, Y. Li^b, P. Franzosi^a, L.J. Giling^b, L. Nasi^a, F. Longo^a, M. Urchulutegui^{a,1},
G. Salviati^a

^aMASPEC-CNR, via Chiavari 18/A, 43100 Parma, Italy

^bUniversity of Nijmegen, Department of Solid State Physics, Nijmegen, Netherlands

Abstract

The structural properties of atmospheric pressure, metal organic vapour phase epitaxy grown GaAs/Ge heterostructures were investigated by transmission electron microscopy and high-resolution X-ray diffraction as a function of substrate misorientation, V to III ratio, growth rate and temperature. A 3° misorientation of the substrate is effective in suppressing the antiphase domains, but only in optimized growth conditions. In the ranges considered, the strain release is influenced more by the misorientation angle and the V to III ratio than by the substrate temperature and the growth rate. The great majority of misfit dislocations are 60° in character; occasionally they react to form edge segments. The misfit dislocations strongly interact with the antiphase boundaries. The contribution of the antiphase domains to strain relaxation is discussed.

Keywords: GaAs/Ge; Antiphase domains; Misfit dislocations; Structural properties

1. Introduction

The increasing interest in GaAs/Ge heterostructures (HSs) is related to their potential application in electronic and optoelectronic devices [1-3]. The high hole mobility of Ge, as well as its narrow band gap, make the GaAs/Ge heterojunction suitable for the fabrication of p-channel field effect transistors, phototransistors and quantum confinement devices. Owing to its high mechanical strength, Ge is an optimized substrate material in terms of the power-to-weight ratio for high-efficiency GaAs/Ge solar cells, especially in space applications. The successful realization of these devices relies on the ability to grow high-quality HSs.

The problems related to the growth of GaAs/Ge are representative of the heteroepitaxy between polar and non-polar and lattice-mismatched semiconductors. The growth of a polar semiconductor on a non-polar one leads, on the layer side of the interface, to the formation of the so-called antiphase domains (APDs) [4], which are the direct consequence of the reduction in

symmetry in passing from the diamond-like structure to zincblende. GaAs can be grown on Ge substrates in two equivalent configurations which differ from each other only in a reversal of the Ga and As positions. Different domains are separated by an antiphase boundary (APB) consisting, in general, of a combination of As-As or Ga-Ga bonds. The lattice mismatch between GaAs and Ge (-7.42×10^{-4} at room temperature) leads to the formation of misfit dislocations (MDs) at the heterointerface when the critical thickness is exceeded. The thermal mismatch between the two materials is negligible.

The aim of this work is to study the structural properties of the GaAs/Ge HSs as a function of the growth conditions and to correlate the characteristics of the defects with the strain relaxation.

2. Experimental details

The growth of GaAs layers was carried out in a horizontal atmospheric pressure, metal organic vapour phase epitaxy (AP-MOVPE) reactor using trimethylgallium (TMG) and arsine (AsH_3) as source materials with a carrier gas of H_2 purified by a Pd diffusion cell. GaAs single epitaxial layers were grown on (001)

¹Permanent address: Departamento Física de Materiales, Facultad de Ciencias Físicas, Universidad Complutense de Madrid, 28040 Madrid, Spain.

vicinal n-type Ge substrates, with a miscut angle ranging from 0° to 4° off (001) towards (111). The growth consisted of two steps: first, an initial growth, which was performed at a growth rate varying between 10 and 30 nm min⁻¹, a temperature of 500 or 700 °C and a V to III ratio from 20 to 60, to a thickness of about 200 nm; the growth conditions were then kept constant for all the samples at a growth rate of 75 nm min⁻¹, a V to III ratio of 13 and a temperature of 700 °C, to a total thickness of about 2.4 μm. The growth conditions are summarized in Table 1: each run consisted of four samples grown at the same time on substrates with different miscutting angle (0°, 2°, 3° and 4°).

The samples were investigated by high-resolution X-ray diffractometry (HRXRD) using Cu K α_1 radiation and a two-crystal-four-reflection monochromator (Ge, 220). Two symmetric 004 and two asymmetric 335 reflection curves were recorded in order to measure the lattice parameters parallel ($a_{||}$) and perpendicular (a_{\perp}) to the (001) plane respectively; as a reference the value $a_{\text{Ge}} = 5.6578 \text{ \AA}$ was used. In the framework of the continuum elasticity theory, the relaxed lattice parameter a_0 was calculated from the relation $a_0 = [(1 + \nu)a_{\perp} + 2\nu a_{||}]/(1 + \nu)$, where the value $\nu = 0.311$ was assumed for the Poisson ratio. Finally, the residual elastic strain parallel to the (001) plane ($\varepsilon_{||}$) was obtained according to the relation $\varepsilon_{||} = (a_{||} - a_0)/a_0$.

Transmission electron microscopy (TEM) investigations were performed on a JEOL 2000FX operating at 200 kV. (001) oriented plan, {110} oriented orthogonal cross-sections of the samples were prepared by conventional mechanochemical procedures and subsequent argon-ion beam thinning at room temperature. As all the layers were thicker than 2 μm, the samples to be examined in plan view were etched from the layer side in order to remove about 1.5 μm so making the imaging of the interfacial region possible.

3. Results

The values of the residual strain $\varepsilon_{||}$ and the full width at half-maximum (FWHM) of the layer Bragg peak are reported in Table 2. The average MD density (d) per unit length corresponding to the measured strain release was calculated according to the formula $d = \delta/b_{\text{eff}}$, where b_{eff} is the effective Burgers' vector component on the plane of the interface (2 Å) and δ is the plastic deformation accommodated by the MDs, supposed to be all 60° type. These values are also reported in Table 2.

In the samples of the same run, the strain relaxation decreases as the misorientation angle increases up to 3° and then increases again. When layers grown under different conditions with the same 3° miscut substrate are

Table 1
Description of the growth conditions: each run consists of four samples (0°, 2°, 3° and 4° off substrates)

Run name	Growth conditions for the first 200 nm			Growth conditions afterwards
	Growth rate (nm min ⁻¹)	V to III ratio	Temperature (°C)	
CT3	10	60	550	Temperature, 700 °C
CT4	30	60	700	V to III ratio, 13
CT5	10	20	550	Growth rate, 75 nm min ⁻¹

Table 2
Summary of the HRXRD investigations (1A = 0° off, 2A = 2° off, 3A = 3° off, 4A = 4° off)

Sample	FWHM (sec arc)	$\Delta a_{ }/a (10^{-3})$	$d (10^4 \text{ cm}^{-1})$
CT3-1A	94	0.53	2.5
CT3-2A	90	0.30	1.5
CT3-3A	46	0.11	0.5
CT3-4A	62	0.18	0.9
CT3-3A	46	0.11	0.5
CT4-3A	46	0.09	0.4
CT5-3A	80	0.41	2.0

compared, no differences in layer relaxation are observed on increasing the initial growth temperature from 550 to 700 °C. This finding indicates that the structural properties are not sensitive to a change in growth parameters over a wide range around the optimum nucleation conditions, especially in this case where an increase in the deposition rate is compensated by an increase in the temperature and a very good value of the V to III ratio is used (see Table 1). A higher value of strain relaxation, which is consistent with the increase in FWHM, is measured when the V to III ratio is three times lower. In conclusion, the strain release is influenced more by the misorientation angle and the V to III ratio than the substrate temperature and growth rate in the ranges considered. The TEM investigations can help to clarify how the strain is accommodated and its correlation with the crystal defects.

The interfacial regions of the samples CT3-1 (0°) and CT3-3 (3°) are shown for comparison in Figs. 1(a) and 1(b) respectively. It is apparent that an increase in the misorientation angle prevents the formation of APDs, which are the irregularly polygonal shaped defects exhibiting dark-white fringe contrast at their boundaries [5]. The APD size is reduced from about 500 to 50 nm or less as the miscut angle changes from 0° to 2°. For larger angles, the APDs are not present in

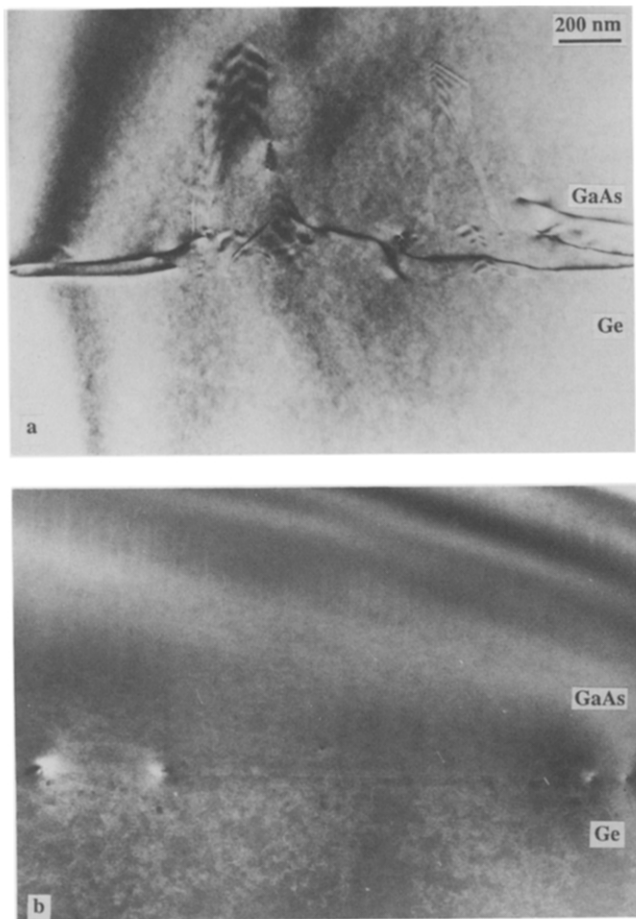


Fig. 1. $\{110\}$ Cross-sectional transmission electron micrographs of GaAs layers grown on: (a) exactly $\langle 001 \rangle$ oriented Ge substrate; (b) 3° off substrate. APBs, which present dark-white fringe contrast in (a), are suppressed by the misorientation. The MDs are well confined in the interface plane in (b), while the presence of APDs forces dislocations to go into the epilayer in (a).

the samples. No remarkable dissimilarities in the shape and size of the APDs between the two different $\langle 110 \rangle$ type orthogonal directions are observed. It is worth noting that all the APBs self-annihilate within 100 nm of the interface, so that the subsequent growth achieves a single domain GaAs layer, which is consistent with the KOH etching results [6].

Investigations carried out on layers deposited with the same growth rate and temperature as the CT3 run, but with a further lowering of the V to III ratio to 10 (not included in the tables) revealed that APDs are also present in 3° off samples. However, these HSs show a very poor structural quality and are not suitable for technological applications.

MDs are present in all the investigated samples as the layer thickness is larger than the critical thickness [7]. From Fig. 1, it is evident that the MDs are strictly confined in the plane of the interface in misoriented

specimens, while the presence of APDs forces MDs to go into the epilayer: in some cases the dislocations run along the APBs.

The very pronounced difference in the defect arrangement between the previous samples is confirmed when they are analysed in plan view, as shown in Fig. 2. In the 0° layer (Fig. 2(a)), the dislocations are distributed in the usual $\langle 110 \rangle$ orthogonal network but, due to the interactions with the APDs, they are no longer extended straight lines. The great majority of MDs have been determined to have a Burgers' vector $a/2 \langle 011 \rangle$ inclined with respect to the interface plane in all the investigated samples. Often MDs abruptly change their original direction and run along the APBs (as already suggested by the cross-sectional analyses): this may be due to the interaction with the elastic strain field [8] or the local charge excess resulting from the As-As and Ga-Ga bonds at APBs. Some MDs stop at the APBs, as evidenced by the arrows in Fig. 2(a), leaving the domain regions dislocation free. The lack of MD segments linking these 'dangling' ends is due to the etching removal of the upper part of the layer, as shown by their oscillating contrast typical of inclined dislocations emerging at the free surface. The APDs projected on the interface plane appear as large irregular closed polygons and their lateral extension is greater than their height. The boundary sheets lie mainly on $\{101\}$ crystallographic orientations, as suggested by the fringes parallel to the $\langle 100 \rangle$ directions on the (001) plane.

MDs are not arranged in the two exactly $\langle 110 \rangle$ type orthogonal arrays in the misoriented samples (Fig. 2(b)), the deviation from orthogonality α being dependent on the misorientation angle φ according to the formula $\alpha = \tan^{-1} [2 \tan(70.5^\circ/2) \tan \varphi]$. As well as the usual interactions between MDs, there are 'low-angle' interactions between dislocations separated by α , which often react to form edge segments with the Burgers' vector in the plane of the interface [9]. An example of these reactions is shown in Fig. 3, where the edge character of some segments is determined by application of the usual contrast extinction rules.

The average density of MDs, obtained from large-area (approximately 3 m^2), plan view, TEM investigations, is the same in the two directions, even if asymmetry is suggested by Fig. 2(b). Actually, a non-uniform distribution of MDs in the sample has been revealed: MDs prefer to align in bands which occur in each direction, as shown by X-ray topography.

The density of MDs measured by TEM is in satisfactory agreement with that calculated by X-ray measurements, for all samples. This result rules out the possibility that APBs have a direct influence on the strain relaxation, but their presence could enhance the generation and/or multiplication of MDs. This fact can

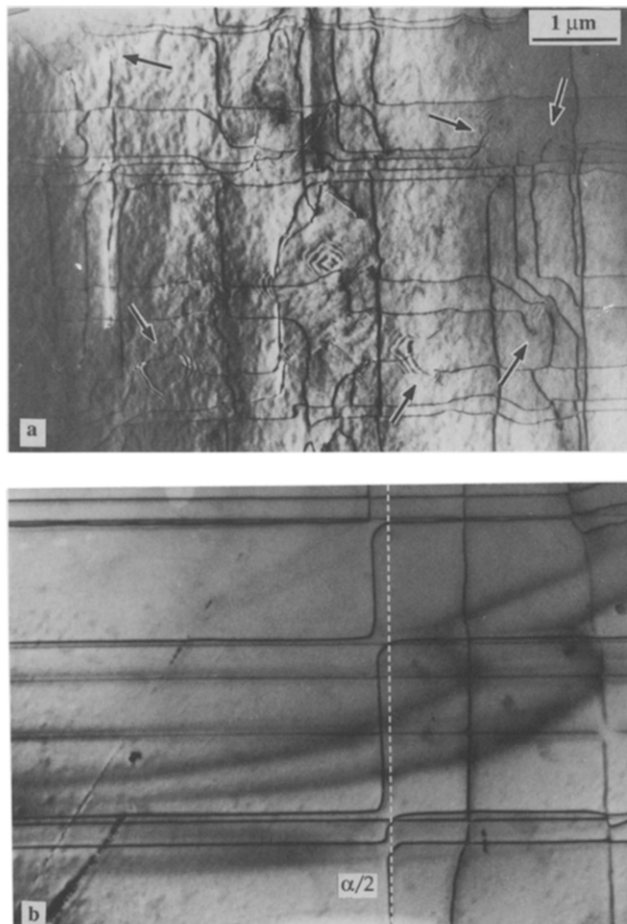


Fig. 2. (001) Plan view TEM of the same samples as in Fig. 1. The difference in the arrangement and density of the MDs is very pronounced. (a) MDs often follow the APBs. (b) The deviation from orthogonality of the dislocation networks, due to the misorient, is indicated (see text for details).

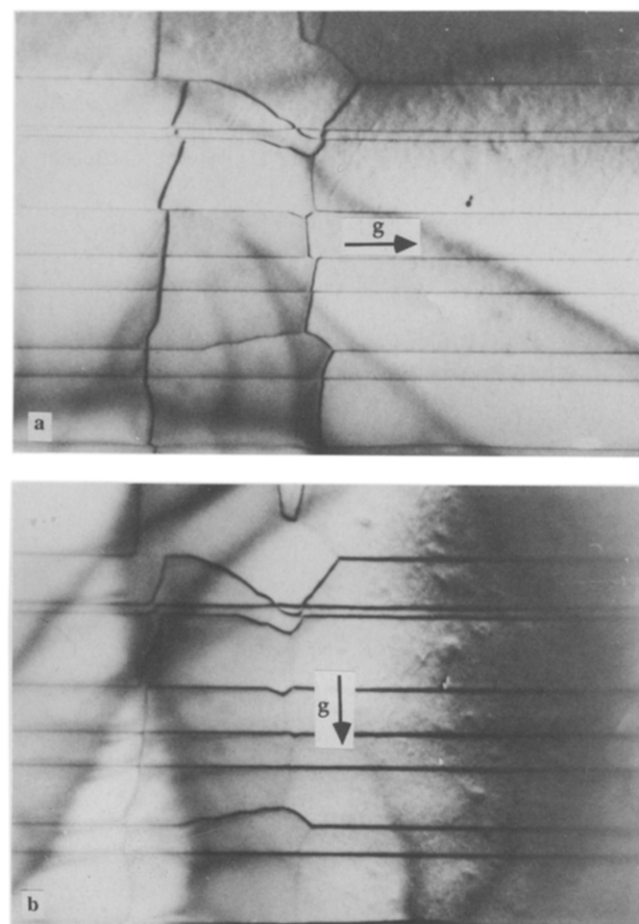


Fig. 3. Part of the dislocation analysis of a 3° misoriented layer. The formation of an edge dislocation segment at a low-angle intersection is shown. (a) $g = 2\bar{2}0$; (b) $g = 2\bar{2}0$.

account for the smaller strain release in misoriented samples. Furthermore, the enhancement of strain relaxation with a decrease in the V to III ratio indicates that a lower V to III ratio leads to the formation of APDs. However, the role of the V to III ratio on the strain relaxation is unclear at the moment and deserves further investigation.

4. Conclusions

The results can be summarized as follows.

(1) A 3° misorientation of the substrate is effective in suppressing the formation of APDs, but only in optimized growth conditions.

(2) In the ranges considered, the strain release is influenced more by the misorientation angle and the V

to III ratio than by the substrate temperature and the growth rate.

(3) The great majority of MDs are 60° in character; occasionally they react to form edge segments. The MDs strongly interact with the APBs.

(4) A direct contribution of the APBs to the strain release can be ruled out.

References

- [1] S. C. Martin, L. M. Hitt and J. J. Rosenberg, *Electron. Device Lett.*, 10 (1989) 325.
- [2] N. Chand, J. Klem and H. Morkoç, *Appl. Phys. Lett.*, 48 (1986) 484.
- [3] J. C. Chen, M. Ladle Ristow, J. L. Cubbage and J. G. Werthen, *J. Electron. Mater.*, 21 (1992) 347.

- [4] D. B. Holt, *J. Phys. Chem. Solids*, 30 (1969) 1297.
- [5] N.-H. Cho, B. C. Cooman, C. B. Carter, R. Fletcher and D. K. Wagner, *Appl. Phys. Lett.*, 47 (1985) 879.
- [6] Y. Li, L. Lazzarini, L. J. Giling and G. Salviati, *J. Appl. Phys.*, in press.
- [7] G. Timò, C. Flores, B. Bollani, D. Passoni, C. Bocchi, P. Franzosi, L. Lazzarini and G. Salviati, *J. Cryst. Growth*, 125 (1992) 440.
- [8] S. N. G. Chu, S. Nakahara, S. J. Pearson, T. Boone and S. M. Vernon, *J. Appl. Phys.*, 64 (1988) 2981.
- [9] P. Kightley and P. J. Goodhew, *Inst. Phys. Conf. Ser.*, 117 (1991) 515.